Cameron J. Ritchie, PhD • Jiang Hsieh, PhD • Michael F. Gard, PhD • J. David Godwin, MD
Yongmin Kim, PhD • Carl R. Crawford, PhD

Predictive Respiratory Gating: A New Method to Reduce Motion Artifacts on CT Scans[1]

PURPOSE: To evaluate a gating system, called predictive respiratory gating (PRG), that reduces motion-induced artifacts on computed tomographic (CT) scans of patients who cannot suspend respiration.

MATERIALS AND METHODS: PRG uses a respiration monitor and a new algorithm to predict when a motionless period is about to occur. It automatically starts scanning so the scan is temporally centered around the motionless period at end inspiration or end expiration. To demonstrate PRG, CT was performed on a motion phantom and a quietly breathing volunteer with and without gating.

RESULTS: Scans of the phantom obtained with PRG contained less motion-induced streaking and blurring than did scans acquired without PRG. Scans of the volunteer gated at end expiration contained significantly less artifact than nongated scans ($P < .03$).

CONCLUSION: PRG reduced motion artifact on scans of a spontaneously breathing volunteer. PRG may be able to reduce motion artifacts on scans of patients unable to suspend respiration.

RESPIRATORY motion during computed tomography (CT) causes artifacts (1,2) that can mimic disease and lead to misdiagnosis (3). These artifacts are particularly frequent on scans of unconscious or pediatric patients who are breathing spontaneously; however, they occur even on scans of conscious, cooperative patients (4). Herein, we describe a scanning method, called predictive respiratory gating (PRG), that reduces respiratory motion artifacts on scans of spontaneously breathing patients. PRG uses a respiration monitor and a new algorithm to predict when a motionless period is about to occur. It then automatically starts scanning so that the scan is temporally centered around the quiescent periods that occur at end inspiration or end expiration.

Other methods for reducing respiratory motion artifacts at CT have been proposed. One method is to use a scanner with a very short (less than 100 msec) scan time; however, such short scan times lead to lower signal-to-noise ratios than those provided with conventional (1 second) scan times (5), and thus conventional scanners are preferred for CT of the chest. Another method is to use a modified filtered back-projection algorithm that corrects for the motion that occurs during scanning; however, this method is limited because a technique for estimating this motion has not been developed (6).

A third method is to use prospective gating to collect segments of the required projection data over several scans in which a different segment of each scan is acquired during a quiescent period in respiratory or cardiac motion (7). This multiple-scan method is not used because it increases the radiation dose and the time required for examination. To our knowledge, PRG with a single scan has not been accomplished with CT because scan times are longer than the quiescent

periods in respiration. Kalender et al (8) acquired full scans during respiration, but they artificially prolonged the quiescent period by mechanically arresting the subject's respiration.

Crawford et al (9) described a PRG method for CT that did not require multiple scans and in which artifacts were reduced even when the scan time was longer than the quiescent period. With computer simulations, artifacts were shown to be reduced when the acquisition of a full scan was timed so the midpoint of the scan coincided with the midpoint of a quiescent period (ie, scanning was "centered" on the quiescent period). Crawford et al recognized scanning must be started before the quiescent period in order to center the scan. Therefore, they proposed that the occurrence of the quiescent period could be predicted by assuming that respiratory motion was periodic. This kind of PRG was not applied on a real scanner.

Recently, slip-ring CT scanners with 1-second scan times have become widely available. The quiescent periods at end expiration (1–2 seconds) and end inspiration (less than 1 second) are approximately equal to these scan times (10). In PRG, we apply the concept of centering the scan on a quiescent period to these faster scanners. To deal with aperiodicities in respiratory motion (11), we replaced the assumption of periodic respiration with an algorithm that predicts when a quiescent period is about to occur and then appropriately times the start of scan acquisition.

MATERIALS AND METHODS

We first characterized respiratory motion in a small group of volunteers to as-

certain the periodicity of spontaneous breathing. Next, we developed a prediction algorithm for computing the time at which quiescent periods would occur. We then combined the prediction algorithm with a respiration monitor and a method for automatically starting the scanner. The resultant system, which we designated PRG, was tested by scanning a motion phantom and a volunteer.

Characterization of Respiratory Motion

We characterized the anteroposterior motion of the chest wall in a small group of volunteers by monitoring the position of the anterior wall of the chest. We used two different motion monitors to track the position of the chest wall. In this part of our study, an infrared rangefinder (model 214 Laser Rangefinder; Spectronics, Beaverton, Ore) was used.

Seven healthy men aged 26–50 years were studied. Each subject lay supine, and a plastic disk was placed on the subject's clothing over the xiphoid process. The rangefinder was placed 10 cm above the disk. Each subject was asked to breath normally and did so for several minutes before data collection was begun. Data collection was begun without the subject's knowledge (to ensure that the measurement was of spontaneous breathing) and was continued for 40 seconds.

Plots of chest-wall position versus time (designated "respiratory waveforms") were generated. For each waveform, the mean and standard deviation of the period of the respiratory cycle, the average difference between adjacent periods, and the maximum difference between periods were computed.

Prediction Algorithm

Preliminary experiments demonstrated that artifacts would not be reduced if the midpoint of a scan occurred more than 0.25 seconds from the midpoint of a quiescent period (Appendix). From our motion characterization, we found that differences between the longest breath and the shortest breath were greater than this time. Therefore, respiratory motion could not be modeled as periodic for the purposes of computing the time at which to start the scanner, and thus the assumption that respiratory motion was periodic was discarded.

Consequently, we developed a prediction algorithm that enabled us to analyze the respiratory waveform and predict the time at which a quiescent period would next occur. The algorithm then computed when the scanner should be started so the scan would be centered around the quiescent period. The prediction algorithm (designated adaptive moving correlation [AMC]) exploits the fact that, whereas the quiescent periods of the respiratory waveform do not occur in a strictly periodic fashion, the shape of the inspiratory or expiratory segment of the waveform is
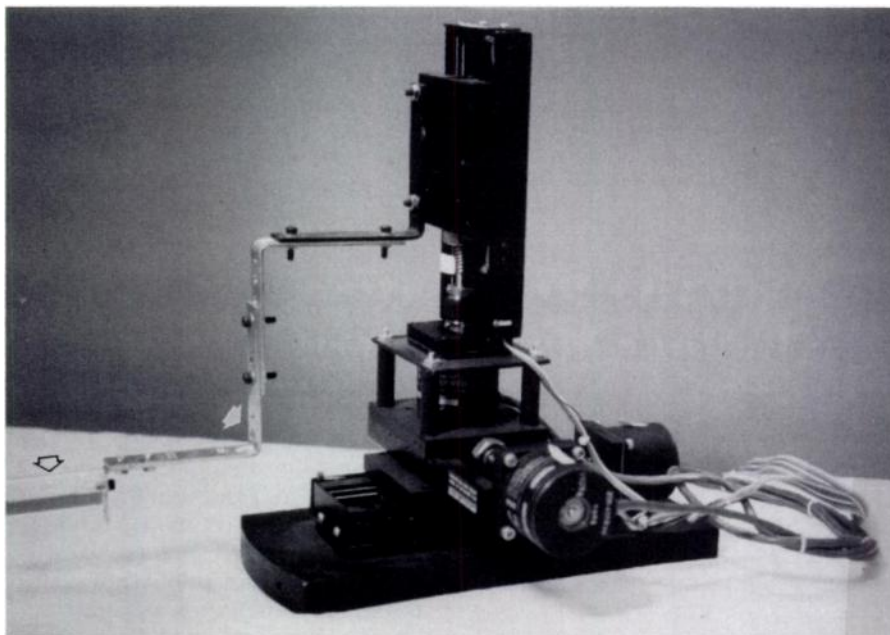
Figure 1. Motion phantom. The phantom consists of three stepping motor and table units. The units are connected so that simultaneous motions along the x, y, and z axes can be specified. The object to be scanned is attached to the long arm (solid arrow). In this photograph, the test object is a plastic cone (open arrow). The motion of each table is controlled by a specially designed circuit board and a computer (not shown).

similar from breath to breath. The algorithm is adaptive in that it adjusts to the waveform being analyzed. The AMC algorithm is described in more detail in the Appendix.

PRG System

We integrated a respiratory monitor with the AMC prediction algorithm and a CT scanner. In this part of the study, we used a linear variable differential transducer ([LVDT] ACT1000C; RDP Electronics, Pottstown, Pa) to track the position of the chest wall. The linear resolution of the LVDT was comparable to that of the infrared rangefinder.

The output of the LVDT was monitored and analyzed by a computer (Sun 3/60; Sun Microsystems, Mountain View, Calif) running the AMC program. The workstation read in the measurements of the chest wall position from the motion monitor, performed the prediction calculations, and then generated the signal to start the scanner. When scanning the motion phantom, we modified the start-scan button on the scanner console (9800 HiLight Advantage; GE Medical Systems, Milwaukee, Wis) so the scanner could be started automatically by the signal from the AMC program. When scanning the volunteer, we did not alter the start-scan button on the scanner (HiSpeed Advantage, GE Medical Systems) because it was not feasible to modify our busy clinical scanner.

Motion Phantom

We tested the PRG system by scanning a motion phantom (12) (Fig 1). The GE 9800 scanner was used because it was available for the modifications needed to control the start of scanning. Respiratory waveforms measured from three of the subjects monitored during the characterization of respiratory motion were reproduced with the motion phantom. The fastest scan time was 2.0 seconds, but scan times on the order of the quiescent period in respiration (1.0 second) were required to test PRG. Therefore, we decreased the frequency at which the motion phantom reproduced the subject's motion to one-fourth that of real respiration, and we proportionately increased the scan time to 4.0 seconds. Therefore, 1.0-second scans were simulated.

A section of dried, inflated human lung was used as the test object, and the probe of the LVDT was placed on the moving arm of the motion phantom. Four-second scans were obtained with 3-mm collimation at 120 kVp and 40 mA and were reconstructed into a 512 × 512 image with a 15-cm field of view. The standard reconstruction algorithm without underscan (also known as the peristalsis option) was used. We first scanned the lung section while it was stationary. Next, we scanned the lung section during inspiration when the phantom velocity was at maximum. Finally, we allowed PRG to control the scanning of the moving section.

Breathing Volunteer

To demonstrate the clinical feasibility of PRG, we performed CT in a healthy 47-year-old male volunteer and had a panel of radiologists evaluate the images. PRG was used retrospectively because we did
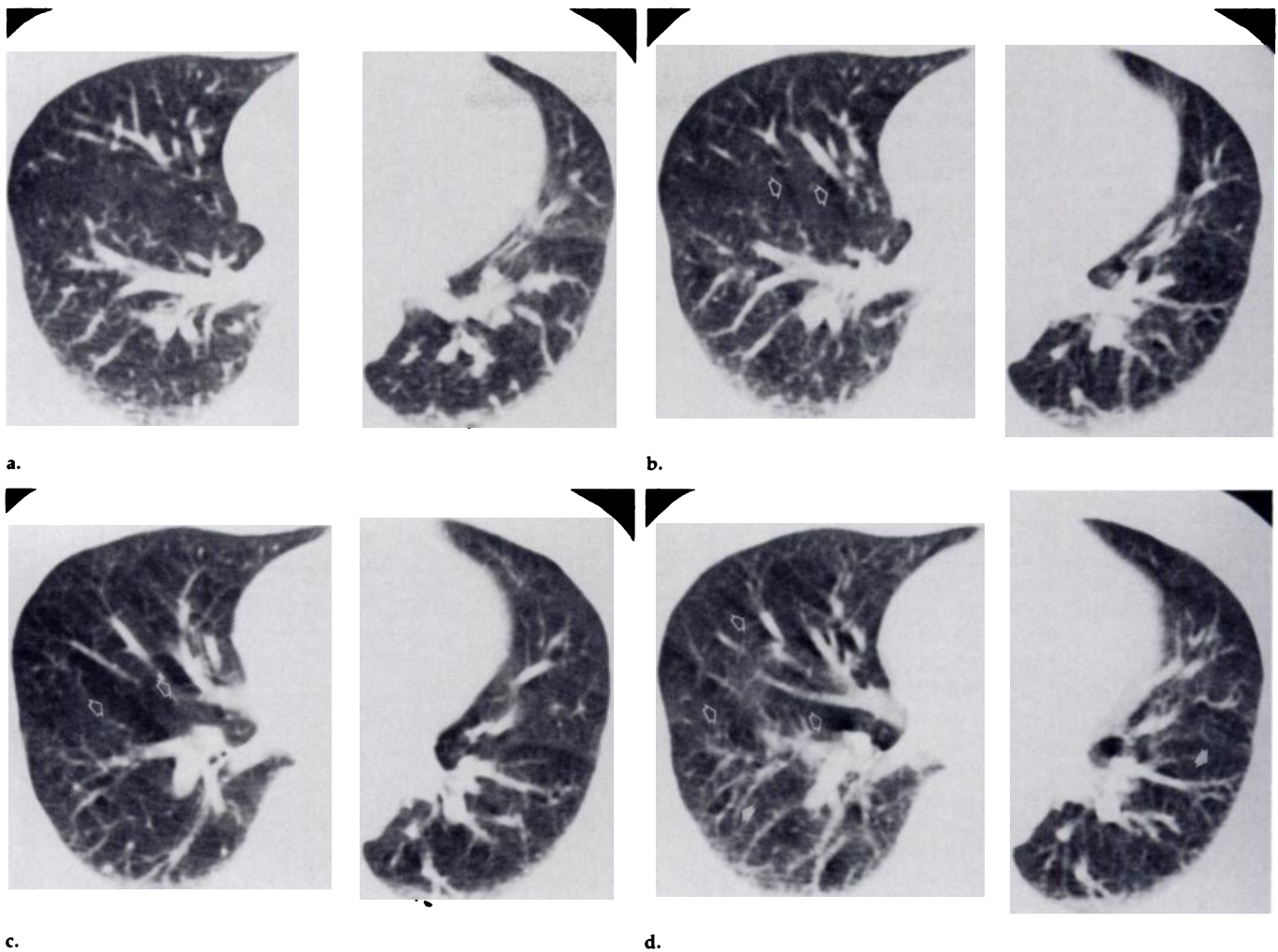
Figure 2. CT scans show grades 0 (a), 1 (b), 2 (c), and 3 (d) artifacts. Motion-induced streaking (open arrows) grows progressively worse from images **b** to **d**. Doubling can be seen in **d** (solid arrows).

not modify the scanner for automatic scanning; however, retrospective gating had the benefit of providing both gated and nongated images for comparison from the same projection set.

The LVDT probe was placed high on the patient's chest to ensure it did not create artifacts, and the volunteer's respiration was measured for 5 minutes. The CT scan was obtained through the lung base, but clear of the diaphragm. Four minutes into the continuous LVDT measurement, the volunteer was scanned continuously for 30 seconds at the same location with 120 kVp, 40 mA, and 5-mm collimation. Images were reconstructed from the 30 seconds of scan data at 0.1-second intervals (291 images total) by using a 512 × 512 matrix with a 48-cm field of view. The standard reconstruction algorithm with and without underscan was used. Low milliamperage was used to limit the dose to the volunteer, but this low value did not affect our results because scans with low milliamperage have been shown to provide chest images of sufficient quality for demonstrating all but low-contrast details (13).

We retrospectively analyzed the respiratory waveform of the volunteer with AMC and computed the start-scan times that would have centered projection acquisition over the quiescent periods. For each start-scan time, we selected the images acquired at the corresponding times from the set of 291 images. This set of selected images represented the images that would have been acquired if PRG had been operating in real time and had started the scanner prospectively. AMC selected images gated at both end inspiration and end expiration.

The volunteer's respiratory waveform was analyzed, and the lengths of the quiescent periods were measured. Quiescent periods were defined as those periods around end inspiration and end expiration in which the motion was less than the minimum detectable motion as determined in a previous study (14).

To determine if the gated images were of significantly higher quality than those acquired without gating, a panel of four experienced chest radiologists scored 50 images (39 nongated, five gated at end inspiration, and six gated at end expiration). Nongated images were chosen randomly from the set of 291 images and represented possible outcomes if a patient who could not suspend respiration was scanned without attention to the phase of the respiratory cycle. A different set of nongated images was selected for each radiologist.

For each radiologist, the 50 images were placed randomly onto three sheets of film and were scored on a scale of 0 (no artifact) to 3 (severe artifact). Each radiologist was also provided with a set of standard images obtained from the same volunteer representing each grade of motion artifact against which to compare the experimental images (Fig 2). These benchmark images had been selected by a fifth radiologist (J.D.G.). Images gated at end inspiration and end expiration were compared with nongated images, and P values were computed for each comparison by using the nonparametric Mann-Whitney test (15).
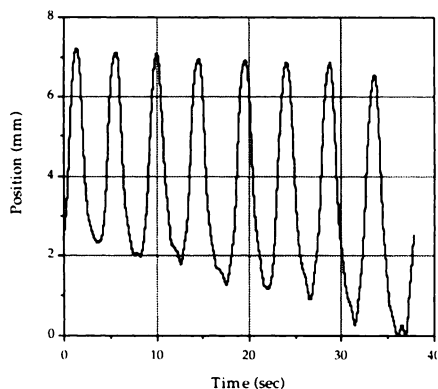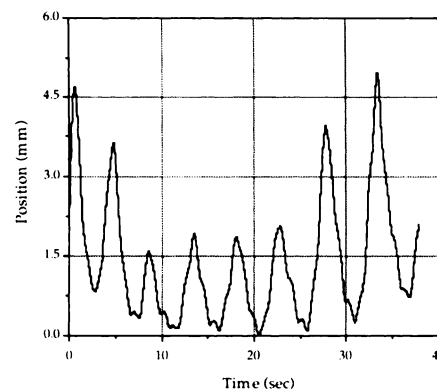
RESULTS

Characterization of Respiratory Motion

In the seven volunteers, plots of respiratory motion demonstrated variations in period and amplitude for each subject. One subject demon-
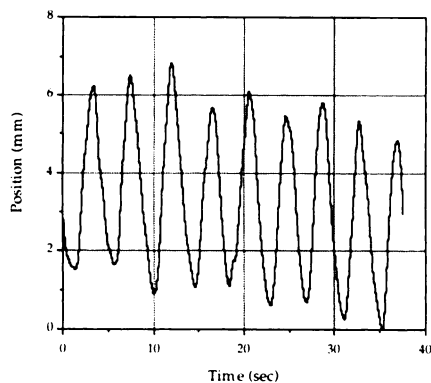
3.   **4.**   **5.**

Figures 3–5. **(3)** Respiration waveform for subject 1. The peaks correspond to inspiration, and the valleys correspond to expiration. Nearly constant period and variable end-inspiratory and end-expiratory chest-wall positions are seen. **(4)** Respiration waveform for subject 2. A nearly constant period and end-inspiratory chest-wall position are seen. **(5)** Respiration waveform for subject 3. A variable period and variable end-inspiratory chest-wall position are seen.

strated nearly periodic motion and moderately variable motion amplitude (Fig 3). In another subject, the period and end-inspiratory chest-wall position were nearly constant over several breaths, but end-expiratory position was not (Fig 4). In a third subject, the period changed, and there was substantial variation in chest-wall position at end inspiration (Fig 5).

The average period of a breath, the standard deviation in the period of a breath, the mean difference between adjacent periods, the difference between the longest and shortest periods, and that difference expressed as a percentage difference of the shortest period were computed for each subject's waveform (Table 1). The standard deviation in the period of a breath ranged from 0.22 to 0.72 seconds. The difference between the longest and shortest periods ranged from 0.52 to 1.78 seconds.

Motion Phantom

The motion phantom was programmed to simulate the breathing of subjects 1, 2, and 3 (Table 1). Images of the lung section obtained without motion were free of artifact and showed expected detail (Fig 6a). Images of the phantom simulating the respiratory motion of subject 1, obtained during the inspiratory portion of the waveform, had substantial motion artifacts, including doubling of small vessels, black voids, and thick white streaks around the high-attenuation structures (Fig 6b). Moving the section in the pattern of the respiratory motion of subject 1 but using PRG to start the scanner resulted in an image with reduced streaking and doubling (Fig 6c). Similar results were

Subject	Mean Period (sec)	Standard Deviation (sec)	Mean $T_n - T_{n-1}$ (sec)	$T_{max} - T_{min}$ (sec)	Max − Min/ Min
1	4.18	0.22	0.18	0.52	12.9%
2	4.59	0.24	0.24	0.67	15.7%
3	4.68	0.58	0.29	1.78	46.1%
4	5.65	0.53	0.61	1.34	27.1%
5	5.35	0.27	0.24	0.69	13.5%
6	7.46	0.72	0.62	1.24	17.6%
7	6.10	0.46	0.46	1.11	20.1%

Table 1
Variations in the Period T of the Respiratory Cycle in Seven Subjects

Note.—max = maximum, min = minimum, T_n = T of breath n, T_{n-1} = T of breath $n - 1$.

obtained when the phantom was programmed to simulate the respiratory motion of subject 2. Use of PRG on the respiratory motion of subject 3 yielded less artifact reduction than for subjects 1 and 2, but the image did contain less artifact than the nongated scan.

Breathing Volunteer

The volunteer's respiration waveform obtained in the 30-second scan period was recorded and analyzed. The volunteer's respiratory rate was about 12 breaths per minute, and the average length of the quiescent periods at end inspiration and end expiration were 0.63 ($\sigma = 0.12$) and 1.42 ($\sigma = 0.28$) seconds, respectively.

The degree of motion artifact on each image was graded by the panel of radiologists. The mean scores of the nongated, gated at end expiration, and gated at end inspiration images were 1.09, 0.11, and 2.23, respectively (Table 2). The use of underscan weighting did not substantially affect the image scores. Each of the four radiologists scored the images gated at end expiration as containing less arti-

fact than the nongated images ($P < .034$) (Table 2). Images gated at end inspiration, conversely, scored significantly worse than nongated images ($P < .052$) (Table 2).

This poor scoring was due to artifacts caused from a coincidental synchronization of cardiac systole with end inspiration. Three of the five end-inspiration scans were obtained at systole, when cardiac motion artifacts are most intense, whereas none of the end-expiration scans were obtained at systole. The occurrence of systole was indicated by the doubled appearance of the left ventricular wall on the gated images. Scans gated at end inspiration in which systole occurred received a mean score of 2.45, while scans at end inspiration in which systole did not occur received a mean score of 1.85.

DISCUSSION

To our knowledge, there has been no effective strategy for reducing artifact on scans of spontaneously breathing patients. There has also been no effective strategy for ensuring that cooperative patients have complied

a.   b.   c.
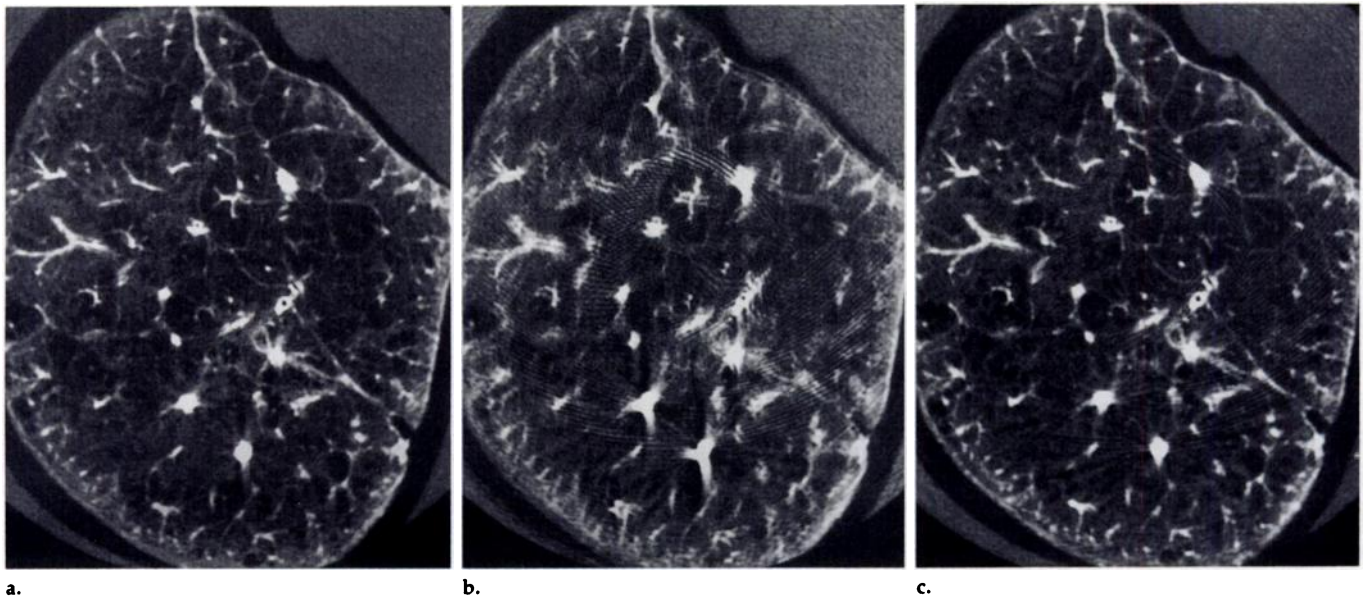
Figure 6. (a) CT scan of dry lung phantom with no motion. (b) CT scan of lung phantom with motion simulating that of subject 1. (c) Optimally gated CT scan of lung phantom with motion simulating that of subject 1.

Table 2
Scores for Gated and Nongated Images

	Mean Scores			P Value	
Radiologist	Nongated	Gated at Inspiration	Gated at Expiration	Nongated vs Gated at Inspiration	Nongated vs Gated at Expiration
1	0.98 (0.77)	1.84 (0.39)	0.00 (0.00)	.010	.002
2	0.89 (0.84)	2.26 (0.73)	0.00 (0.00)	.004	.006
3	1.34 (1.06)	2.36 (0.56)	0.38 (0.49)	.052	.034
4	1.15 (1.00)	2.44 (0.38)	0.05 (0.12)	.007	.001
Mean	1.09	2.23	0.11	...	...

Note.—Numbers in parentheses are standard deviations.

with the scanner technician's instruction to hold their breath. We have demonstrated that scans with substantially reduced artifact can be obtained from spontaneously breathing patients by using PRG. Additionally, the use of PRG could eliminate the need for patients to hold their breath. Finally, PRG could be used to improve registration of contiguous scans for volume display.

The PRG system consists of a respiration monitor, software, and modifications to the scanner start-scan button. Because PRG requires only minimal scanner modifications, it should be applicable to scanners with sufficiently short scan times so an entire scan can be acquired during a quiescent period.

PRG was performed in both a moving lung slice and a volunteer. PRG scans of the moving lung slice demonstrated reduced motion artifact compared with nongated scans for two of the three subjects' respiration waveforms. PRG scans gated at end expiration demonstrated reduced motion artifact compared with nongated scans. Although radiologists generally prefer to acquire CT scans at full inspiration, we found that images gated to end tidal volume adequately preserved lung detail and were superior to nongated images even though the nongated images were obtained at greater lung volumes.

We were unable to gate all the phantom scans appropriately with PRG because we performed our phantom experiments on a scanner with a long scan time (4.0 seconds) and a long scanner delay (2.26 seconds). (Scanner delay is the time between pressing the start-scan button and the start of projection acquisition.) These long delays cause errors in the prediction of the time the quiescent period in breathing will occur. Although prediction accuracy suffers somewhat when using a scanner with a long scan time and a long scanner delay, some artifact reduction can still be obtained by using PRG with this type of scanner, as shown by our results with subjects 1 and 2.

The ability of PRG to reduce motion artifacts depends on the respiration waveform of the patient. We tested PRG on waveforms with respiratory periods as short as 4.18 seconds. For respiratory periods much shorter than this, PRG scans will not demonstrate as much motion artifact reduction because the quiescent periods will be necessarily shorter. However, because normal respiration has a period of approximately 4 seconds (10), the PRG system should perform satisfactorily with most patients.

We did not address artifacts caused by cardiac motion. Cardiac motion artifacts could be eliminated by gating both on the cardiac cycle and on the respiratory cycle (9); however, the quiescent period in cardiac motion (at end diastole) is too short for conventional scanners with 1-second scan times. Fortunately, cardiac motion is only a problem when scanning near the diaphragm. Cardiac motion is not as great a problem for scans of the abdomen or the upper chest.

For PRG to gain wide clinical acceptance, a clinically suitable respiration monitor is needed. The monitor must be noninvasive and easy to use and should not cause artifacts if it intersects the scan plane. The infrared and LVDT respiration monitors used in this study were easy to use. They were also able to monitor the chest motion from well outside the scan plane because the AMC algorithm

does not base its prediction on the amplitude of the respiration signal.

We report a promising new method for scanning patients who do not suspend breathing. Artifacts were significantly reduced in scans gated at end expiration in a volunteer. These preliminary results need confirmation in a larger number of subjects, including patients who cannot suspend breathing for a variety of reasons.

APPENDIX

Determination of Maximum Error

In PRG, the timing of the start of scan acquisition is based on the time a quiescent period is predicted to occur. Crawford et al (9) proposed this prediction could be made by assuming respiration is periodic over the course of several breaths. To ascertain if this assumption was valid, we determined how much time could separate the midpoint of the quiescent period and the midpoint of the scan before artifacts began to appear on images. This time is designated the allowable error.

To determine the allowable error, a plastic peg (1-cm diameter) was scanned 16 times while it moved in a pattern that reproduced the motion of a single cycle of respiratory motion as measured in subject 1 (Table 1). The midpoints of the 16 scans were equally spaced in time through the 4-second respiratory cycle. Streaking artifacts on the images of the peg were quantitated by measuring the standard deviation in a region of interest placed far from the peg on each image. Images that were optimally centered on end inspiration or end expiration demonstrated minimal standard deviation measurements. The allowable error was equal to the amount of time that separated these optimally centered images from the first image that contained visible motion artifacts.

The maximum errors for expiration and inspiration were 0.5 and 0.25 seconds, respectively. From Table 1, the differences between the shortest period and the longest period in respiratory motion ranged from 0.52 to 1.78 seconds and thus ex-

ceeded the maximum errors for both inspiration and expiration. Therefore, reliably gated images at either end inspiration or end expiration could not be obtained if periodicity was assumed when performing start-scan time calculations.

Description of AMC

The AMC algorithm computes the time at which quiescent periods in the respiratory waveform will occur by computing the correlation coefficient between an initial segment F and the most recent measurements G of the respiratory waveform, where F and G are vectors. A correlation coefficient equal to 1 indicates that the vectors are identical, while a coefficient of zero indicates that the vectors are unrelated.

We first measure the position of the chest wall for several breaths. The vector G (called the kernel) is formed from this initial block of data and is equal to those values of the waveform that immediately preceded the quiescent period. The last point in the kernel, k_{end}, is positioned one-half the scan time plus the scanner-delay time before the midpoint of the quiescent period. A vector F is formed each time a new measurement is returned from the respiration monitor, and a correlation coefficient is computed between F and G. When the correlation coefficient becomes greater than 0.99, it indicates that the point corresponding to k_{end} in the next respiratory cycle has just been measured, and thus AMC outputs a start-scan signal.

When a start-scan signal is output, a new kernel is formed by averaging F with G. This averaging allows AMC to adapt to changes in the breathing pattern over time. The averaging step is constrained so only measurements representative of normal respiration are averaged into the new kernel. This constraint ensures that faulty measurements (ie, measurements obtained during a cough or sneeze) are filtered out. ∎

References

1. Shepp LA, Hilal SK, Schulz RA. The tuning fork artifact in computerized tomography. Comput Graph Imaging Processing 1979; 10:246–255.

2. Mayo JR, Müller NL, Henkelman RM. The double-fissure sign: a motion artifact on thin-section CT scans. Radiology 1987; 165:580–581.
3. Tarver RD, Conces DJ, Godwin JD. Motion artifacts on CT simulate bronchiectasis. AJR 1988; 151:1117–1119.
4. Dupuy DE, Costello P, Ecker CP. Spiral CT of the pancreas. Radiology 1992; 183: 815–818.
5. Gould RG. Principles of ultrafast computed tomography: historical aspects, mechanism of action, and scanner characteristics. In: Stanford W, Rumberger JA, eds. Ultrafast computed tomography in cardiac imaging: principles and practice. Mount Kisco, NY: Futura, 1992; 1–15.
6. Ritchie CJ, Kim Y, Crawford CR, Godwin JD. CT motion artifact correction using pixel-specific back-projection. Proc IEEE Eng Med Biol Soc 1992; 14:1782–1783.
7. Moore SC, Judy PF, Garnic JD, Kambic GX, Bonk F, Cochran G. Prospectively gated cardiac computed tomography. Med Phys 1983; 10:846–855.
8. Kalender WA, Fichte H, Bautz W, Skalej M. Semiautomatic evaluation procedures for quantitative CT of the lung. J Comput Assist Tomogr 1991; 15:248–255.
9. Crawford CR, Godwin JD, Pelc NJ. Reduction of motion artifacts in computed tomography. Proc IEEE Eng Med Biol Soc 1989; 11:485–486.
10. Buikman D, Helzel T, Röschmann P. The RF coil as a sensitive motion detector for magnetic resonance imaging. Magn Reson Imaging 1988; 6:281–289.
11. Vannier MW. Respiratory gating by impedance plethysmography. J Nucl Med 1984; 25:1142–1143.
12. Ritchie CJ, Peterson E, Yee D, Kim Y, Godwin JD, Crawford CR. A 3-D motion control system for simulation of CT motion artifacts. Proc IEEE Eng Med Biol Soc 1989; 11:487–488.
13. Naidich DP, Marshall CH, Gribben C, Arams RS, McCauley DI. Low-dose CT of the lungs: preliminary observations. Radiology 1990; 175:729–731.
14. Ritchie CJ, Godwin JD, Crawford CR, Stanford W, Anno H, Kim Y. Minimum scan speeds for suppression of motion artifacts in computed tomography. Radiology 1992; 185:37–42.
15. Zar JH. Biostatistical analysis. Englewood Cliffs, NJ: Prentice-Hall, 1974; 109–114.